Life Sciences 238 (2019) 116956

Contents lists available at ScienceDirect

Life Sciences

journal homepage: www.elsevier.com/locate/lifescie

Rheumatoid arthritis induces enteric neurodegeneration and jejunal inflammation, and quercetin promotes neuroprotective and anti-inflammatory actions

Gleison Daion Piovezana Bossolani[a], Bruna Thais Silva[a], Juliana Vanessa Colombo Martins Perles[a], Mariana Machado Lima[a], Flávia Cristina Vieira Frez[a], Sara Raquel Garcia de Souza[a], Camila Caviquioli Sehaber-Sierakowski[a], Ciomar Aparecida Bersani-Amado[b], Jacqueline Nelisis Zanoni[a,*]

[a] Department of Morphological Sciences, Universidade Estadual de Maringá, 87020-900, Maringá, Paraná, Brazil
[b] Department of Pharmacology and Therapeutic, Universidade Estadual de Maringá, Máringá, Paraná, Brazil

ARTICLE INFO

Keywords:
Enteric nervous system
Glia
Quercetin
Rheumatoid arthritis

ABSTRACT

Aims: The aim of our study was to study the pathological mechanisms induced by the rheumatoid arthritis (RA) on the Enteric Nervous System (ENS).

Main methods: We evaluated the effect of the chronic arthritis and its treatment with 50 mg/kg quercetin alone (AQ) and combined with 17.5 mg/kg ibuprofen (AIQ) for 60 days on neurons, glial cells and intestinal wall. Other groups were used: control (C), arthritic (A) and arthritic treated with 17.5 mg/kg ibuprofen (AI). After 60 days, the jejunum was removed and processed for immunohistochemical techniques. Immunostainings were performed for HuC/D and S100 (myenteric and submucosal plexuses), and GFAP (only myenteric plexus), while immunolabeling for CD45 and CD20 lymphocytes was performed using cryosections. Western blot was performed for GDNF, S100 and GFAP.

Key findings: A group yielded a remarkable density decrease of the neurons and glial cells with morphometric changes in the myenteric and submucosal plexuses, reduction of the GDNF expression and GFAP-related parameters (GFAP expression, occupancy area and GFAP-expressing glial cells) and intestinal inflammation and atrophy of the mucosa and intestinal wall. AQ group substantially reversed most of these effects, except for intestinal atrophy of the jejunum. The AI and AIQ groups displayed lower beneficial results than AQ for parameters related to the neurons and glial cells, although AIQ did not prevent the inflammation of the mucosa.

Significance: The severe chronic rheumatoid arthritis induced severe effects on ENS and mucosa, and quercetin treatment continues to be an important antioxidant supplement preventing the progression of the RA severity.

1. Introduction

Rheumatoid arthritis (RA) is an inflammatory and autoimmune disease that causes bone and cartilage destruction [1,2]. RA is also considered a multisystemic disease that affects extra-articular organs (e.g. skin, eye, heart, lung, kidneys, heart, blood vessels, nervous and gastrointestinal systems) [3–6] and is more frequent in patients with severe and progressive disease associated with increased mortality [3]. Currently, 1-2% of the worldwide population has been affected by the RA [2,7] and 40% of the arthritic patients may develop extra-articular manifestations either at the onset or during progression of the disease [3]. The presence of autoantibodies, increased oxidative stress and production of pro-inflammatory cytokines underlies the pathophysiology of the RA [7–9].

Few studies have been performed to confirm changes on enteric glial cells (EGC) and neurons of the Enteric Nervous System (ENS) induced by RA, although presence of peripheral neuropathy has reported in patients with RA [10–12]. In a RA model, jejunal and ileal segments of arthritic rats induced by complete Freund's adjuvant displayed no quantitative changes on enteric neurons, although morphometric changes were observed in the myenteric neurons [13]. The gastrointestinal tract (GIT) is innervated by a complex nervous network and

* Corresponding author. Universidade Estadual de Maringá Departamento de Ciências Morfológicas, Laboratório de Plasticidade Neural Entérica, Avenida Colombo, 5790, Bloco O33, CEP, 87020-900, Maringá, PR, Brazil.
E-mail address: jnzanoni@uem.br (J.N. Zanoni).

https://doi.org/10.1016/j.lfs.2019.116956
Received 21 August 2019; Received in revised form 8 October 2019; Accepted 10 October 2019
Available online 14 October 2019
0024-3205/

distributed in myenteric and submucosal plexuses [14,15]. These EGC and neurons are involved in the intestinal functional homeostasis [16–22].

The EGC display a crucial structural role to neurons and their survival, maintenance and function [19], and these cells form a network that consists in intermediate gliofilaments protecting the neurons [19,21]. EGC are also present in non-ganglionated plexuses and mucosa [21,23–26]. Mature glial cells richly express the glial fibrillary acidic protein (GFAP) in their intermediate filaments, which may be up- or downregulated during differentiation and inflammatory conditions [20]. Furthermore, EGC also have a calcium binding protein (S100) present in the cytoplasm and/or nucleus that regulates specific intracellular signaling pathways (e.g. regulation of the calcium homeostasis, cytoskeletal stability and apoptosis induction) [26]. S100 exerts a metabolic support to ENS and displays crucial role in enteric neurotransmission, secretion, nutrient uptake, motility, immune and inflammatory processes [26,27]. Studies have confirmed that EGC avoid the neuronal death by the release of the glial cell derived neurotrophic factor (GDNF), which is produced by the EGC in pathological and neuropathy processes. The key function of the GDNF is the maintenance and survival of the neurons reducing the neuronal death by apoptosis and inflammation [16,28–30].

The pharmacotherapy of the RA is based on five main classes of medicines: analgesics, non-steroidal anti-inflammatory drugs (NSAIDs), glucocorticoids, nonbiologic and biologic disease-modifying antirheumatic drugs (DMARS) [31]. Given the absence of cure by the RA treatment, the aim of the antirheumatic therapy is to alleviate the symptoms and avoid joint and organ damages [2]. Quercetin, a potent antioxidant, is commonly found in fruits and vegetables and exerts several biological activities (e.g. inflammatory, anticancer, hepatoprotective, antidiabetic and antibacterial properties), including anti-rheumatic actions [32–35].

The quercetin has showed protective activities protecting the EGC and neurons from cellular death by diseases [36–40], and anti-rheumatic effects mostly occur due to its antioxidant and anti-inflammatory properties [33–35]. Based on its biological properties, this study aimed to assess the effect of quercetin alone (50 mg/kg) and combined with ibuprofen (17.5 mg/kg) on enteric neurons, EGC and jejunal lymphocytes.

2. Methods

2.1. Experimental design

The experimental study was performed in accordance with the international guidelines of ethical regulation and previously approved by the Committee of Ethical Conduct on the Use of Animals in Experimentation (CEAE) of the State University of Maringá - Paraná - Brazil (UEM), CEUA nº 4462180216.

A group of twenty-five 56-day-old male Holtzman rats (*Rattus norvegicus*) was housed in polypropylene boxes with following dimensions: length (40 cm), width (33 cm) and height (17 cm). The rats received food and water *ad libitum* and were kept under constant environmental conditions of temperature (22° ± 2 °C) and illumination (cycle 12 h light/12 h dark). All animals received standard balanced Nuvital feed (Nuvital®, Colombo, PR, Brazil).

The experimental groups consisted of 5 groups with 5 animals per group randomly distributed: control (C), adjuvant-induced arthritic (A), adjuvant-induced arthritic treated with 17.5 mg/kg ibuprofen (AI), adjuvant-induced arthritic treated with quercetin (50 mg/kg) (AQ) and adjuvant-induced arthritic treated with quercetin (50 mg/kg) and ibuprofen (17.5 mg/kg) (AIQ).

The quercetin was administered at the dose of 50 mg/kg diluted in water and ibuprofen at a dose of 17.5 mg/kg was diluted in carboxymethylcellulose (CMC) solution. The CMC was used as a pharmacological inert diluent in order to dissolute ibuprofen in water [41–44]. For this reason, additional groups only treated with vehicle (CMC or water) was not performed in our study since the main objective of this research was to assess the arthritis-induced effects on ENS and joint inflammation, and the treatment impact of the quercetin alone and combined with ibuprofen.

2.2. Induction of rheumatoid arthritis

The induction of the arthritic model was obtained by the intradermal injection of 0.1 ml complete Freund's adjuvant (CFA) of 5% heat-killed suspension of *Mycobacterium tuberculosis* into the right hind paw of each animal [45,46]. The negative control (non-arthritic rats) also received an intradermal injection that only contained 0.1 mL of the vehicle (mineral oil; Nujol®, Schering-Plow, São Paulo-Brazil).

To confirm the establishment of arthritic disease, the left paw edema was measured on days 0 (induction day), 1st, 3rd and 6th of the experiment using a digital hydro plethysmograph, expressed by the increase in the volume (μL) of the left paw compared to the initial volume.

2.3. Treatment

The experimental treatment was daily carried out by gavage during 60 days. The dose of 50 mg/kg of the quercetin was chosen based on previous effects of the quercetin supplementation in water at a dose of 200 mg/kg [37,38] and 40 mg/kg [36,39]. In this study, the dose of 17.5 mg/kg of the ibuprofen was selected in line with previous studies as a positive control and conventional anti-inflammatory drug used by the humans [41–44].

2.4. Collection and processing of samples

After 60 days, the animals were maintained for a 12 h fasting period. Afterwards, all rats were intravenously administered with vincristine (0.5 mg/kg body weight - Eurofarma®, Brazil) using penile vein 2 h before euthanasia in order to block the formation of the cellular microtubules. After 2 h, the animals were intraperitoneally injected with thiopental (40 mg/kg body weight - Abbott Laboratories, Chicago, IL, USA), the celiotomy was performed to collect the entire small intestine and its length was measured. The jejunal segment was removed and then, opened along the mesenteric border and its width was also measured. The total area of the small intestine was determined by the multiplication of the width by the length, expressed in cm^2. These opened tissues were incubated in Zamboni's fixative for 18 h [47] and subsequently, rinsed in phosphate-buffered saline (PBS; 0.1 M, pH 7.4). Afterwards, the intestinal samples were incubated in a 18% sucrose solution (w/v) for 24 h and then, immersed in a solution of optimum cutting temperature (OCT) and frozen −80 °C. Subsequently, the histological sections of 10 μm thickness were placed on microscope slides using a cryostat for the subsequent immunostaining techniques of the intestinal wall [48].

The non-opened jejunal samples were firstly rinsed in PBS and filled with Zamboni's solution and then, incubated for 18 h at 4 °C. Afterwards, the samples were opened along the mesenteric border and successively rinsed in 80% alcohol to remove the fixative completely. Subsequently, the jejunal samples were sequentially dehydrated using increasing concentrations of alcohols (95% and 100%), diaphanized in xylol and then, rehydrated in descending concentrations of alcohols (100%, 90%, 80% and 50%). After that, the intestinal tissues were stored in PBS containing 0.08% sodium azide (Sigma-Aldrich, Inc., St. Louis, MO, USA) at 4 °C until the subsequent immunohistochemical procedures. These intestinal tissues were cut into small pieces of approximately 1 cm^2 and microdissected using a stereomicroscope Stemi DV4 (Zeiss, Jena, Germany) in order to obtain thin specific layers where are found the muscular tunica and the submucosa. The evaluation of the ganglionated plexuses of the ENS consisted in the removal of the

Table 1
Primary and secondary antibodies used in immunohistochemical and Western blot reactions.

Primary antibody	Source	Dilution (IHC)	Dilution (WB)
Monoclonal produced in mouse anti-HuC/D	Molecular Probes, Invitrogen, OR, USA	1:300	—
Monoclonal produced in rabbit anti-S100	Santa Cruz Biotechnology, USA	1:200	1:1000
Monoclonal produced in mouse anti -GFAP	Santa Cruz Biotechnology, USA	1:200	1:1000
Policlonal produced in goat anti-GDNF	Santa Cruz Biotechnology, USA	—	1:1000
Monoclonal produced in mouse anti-GAPDH	Santa Cruz Biotechnology, USA	—	1:1000
Policlonal produced in mouse anti-CD45	Molecular Probes, Invitrogen, OR, USA	1:300	—
Policlonal produced in mouse anti-CD20	Molecular Probes, Invitrogen, OR, USA	1:300	—
Secondary antibody			
Alexa fluor 488 (donkey anti-rabbit)	Molecular Probes, Invitrogen, OR, USA	1:200	—
Alexa fluor 568 (goat anti-mouse)	Molecular Probes, Invitrogen, OR, USA	1:500	—
Alexa fluor 488 (donkey anti-mouse)	Molecular Probes, Invitrogen, OR, USA	1:300	—
HRP-conjugated goat anti-rabbit	Novex, Invitrogen, USA	—	1:1000
HRP-conjugated rabbit anti-mouse	Novex, Invitrogen, USA	—	1:2000
HRP-conjugated mouse anti-goat	Novex, Invitrogen, USA	—	1:2000

IHC = immunohistochemistry; WB = Western blot; HRP = horseradish peroxidase.

tunica mucosa to obtain the myenteric plexus. The submucosal tissue was obtained by scraping of the mucosal layer for the exposure of the submucosal plexus [47].

2.5. Study on ENS and frozen cryosections

2.5.1. Immunohistochemistry for the HuC/D, S100 and GFAP

The both microdissected membranes were rinsed in PBS (2 × 10min) that contained 0.5% Triton X-100 (T8532; Sigma-Aldrich, Saint Louis, MO - USA). Afterwards, the jejunal samples were incubated in blocking solution containing PBS (0.1 M, pH 7.4), 2% BSA (bovine serum albumin, A9647 - Sigma, Saint Louis, MO - USA), 10% donkey serum and 0.5% Triton X-100 for 1 h. After blocking, the tissues were incubated in a new solution that contained the same formula used in the blocking solution adding the following primary antibodies: anti-HuC/D and anti-S100 (double immunostaining) [47] and GFAP [49] (single immunolabeling) (Table 1) for 48 h at room temperature (RT). After antibody incubation, the intestinal segments were rinsed in a solution that contained PBS and 0.5% Triton X-100 (2 × 10 min). Subsequently, the intestinal membranes were incubated in the corresponding secondary antibody (Table 1) for 2 h at RT. Subsequently, the jejunal tissues were rinsed in PBS (2 × 10 min), placed on slides with buffered glycerol with PBS (9:1) and stored at 4 °C. For the negative control, the primary antibody was not used. The GFAP immunostaining was only performed in myenteric plexus. Furthermore, the GFAP immunolabeling was counterstained with DAPI to visualize the nuclei.

2.5.2. Single immunohistochemistry for CD45 and CD20 lymphocytes using frozen histological sections

Frozen histological sections, previously obtained from the cryostat and placed on microscope slides, were washed in PBS with Triton X-100 (0.5%) (2 × 10 min). After rinsings, the blocking was performed with PBS, 2% BSA, 10% donkey serum and Triton X-100 (0.5%) for 1 h. After that, the jejunal samples were incubated in a solution with anti-CD20 and anti-CD45 primary antibodies produced in mice for 48 h at RT (Table 1). After incubation, risings were performed using PBS (2 × 10 min) and then, the samples were incubated using the Alexa Fluor anti-mouse 488 secondary antibody (1:500) for 2 h at RT (Table 1). After rinsing in PBS, the slides were mounted with buffered glycerol [50]. For the negative control, the primary antibody was omitted.

2.5.3. Image acquisition

The images were obtained by a Moticam® 2500 5.0 Mega Pixel high resolution camera (Motic China Group Co., Shanghai, China) coupled to an Olympus fluorescence optical microscope® BX40 (Olympus Co., Japan), transferred to microcomputer through the software Motic Images Plus® 2.0 ML (Motic China Group Co., Shanghai, China) and recorded. For double labeling for S100 and HuC/D, 30 images were captured using a 20× objective lens, whereas 20 images were obtained for GFAP using a 40× objective lens. For the immunostaining for lymphocytes (CD45 and CD20) using frozen histological sections, a 10× objective lens was used and a number of images was acquired until obtaining 30 villi.

2.5.4. Correction of neuronal and glial density

The cellular correction was used to avoid morphoanatomical alterations that occur in several pathophysiological conditions and may interfere in the results of the cellular density of the neurons and EGC (cell dispersion or concentration) [51,52]. Comparing the mean areas of the arthritic groups (A, AI, AQ and AIQ) to the control group, a correction factor was calculated by the ratio between the areas of the intestinal segments in the arthritic groups and the control group (Table 2). The cellular density of each arthritic group in the

Table 2
Volume of left paw edema obtained by a hydroplethysmograph, mean area of the jejunum and the correction factor used to correct the neuronal and glial density. Experimental groups: control (C), arthritic (A), arthritic treated with ibuprofen 17.5 mg/kg (AI), arthritic treated with quercetin 50 mg/kg (AQ) and arthritis treated with 50 mg/kg quercetin and 17.5 mg/kg ibuprofen (AIQ).

Groups	Paw edema (μL)				Jejunal area (cm^2)	FC
	Day 0	Day 1st	Day 3rd	Day 6th		
C	132 ± 2	132 ± 2	135 ± 2	137 ± 3	186 ± 15	-
A	126 ± 2	299 ± 18[a]	333 ± 16[a]	349 ± 17[a]	168 ± 7[a]	0.9
AI	120 ± 2[a]	257 ± 12[a,b]	287 ± 20 [a,b]	283 ± 19[a,b]	173 ± 8	0.93
AQ	124 ± 2[a]	255 ± 10[a,b]	293 ± 13 [a,b]	314 ± 10[a,b]	166 ± 5[a]	0.89
AIQ	123 ± 1[a]	230 ± 5[a,b]	255 ± 10 [a,b]	285 ± 8[a,b]	162 ± 7[a]	0.87

FC = correction factor. [a] = significant in comparison to the control group ($p < 0.05$) and [b] = significant in comparison to the arthritic group ($p < 0.05$). Data are expressed as mean ± standard error. n = 5 animals per group.

quantitative analysis was multiplied by this correction factor.

2.5.5. Quantification and morphometry of the S100-IR glial cells and HuC/D-IR enteric neurons of the myenteric and submucosal plexuses

For the immunohistochemical techniques for HuC/D and S100, the analysis was performed in the intermediate region of the jejunum. The neuronal and glial populations of each image were quantified using the Image-Pro® Plus version 4.5 program (Media Cybernetics Inc., Rockville, MD, USA) [47]. The results were expressed as cells per cm^2, which were obtained considering the measurement of the image area and correction of the intestinal area for the calculation of the neuronal and glial density. For the morphometric analysis, the area of 100 cells (S100-IR EGC and HuC/D-IR neurons) per animal was measured using the same program [47]. The morphometric results were expressed in μm^2.

2.5.6. Quantitative analysis of glial cells expressing the GFAP protein and the occupancy area by the GFAP-IR intermediate filaments

The quantification of the GFAP-expressing EGC [53], which is observed surrounding the glial cellular body stained with DAPI, was performed using Image-Pro® Plus software version 4.5. Analyzing 20 parts of the nervous ganglia present in intermediate region of the jejunum, the occupancy area by the GFAP-IR intermediate filaments was measured using ImageJ® software version 1.43° (NIH), where the images were converted to 16 bits and a binarization function was used to remove the background intensity [54].

2.5.7. Quantification of CD45 and CD20 lymphocytes of intestinal mucosa and assessment of total thickness and villus height of jejunum

For the quantification of the CD45 and CD20 lymphocytes, 30 villi were counted per animal using Image-Pro® Plus version 4.5 Software [48]. The results were expressed as a mean of lymphocytes/villus.

For the morphometric analysis of histological sections of the jejunum, 30 units of the villi and total wall thickness of jejunum were measured [47]. The length of the villi comprises from the extension of the crypt-villus junction until the top of the villus. The total height of the intestinal wall includes the extension of the intestinal wall from the serous tunic until the top of the villi.

2.6. Western blot

The jejunal protein expressions for the GFAP, GDNF and S100 proteins were evaluated. After celiotomy, the jejunal segments were repeatedly rinsed in Krebs-Ringer buffer (pH 7.4). The intestinal tissues were centrifuged for 10 min at $10.000 \times g$ using a homogenization buffer [50 mM Tris HCl, pH 7.4, 600 mM NaCl, 1 mM ethylenediaminetetracetic acid (EDTA) Sigma-Aldrich] and the supernatant was collected and frozen (−80 °C). Total protein concentration per sample was measured using the Bradford protein assay (Bio-Rad, Hercules, CA, USA) [55]. Afterwards, the proteins were separated using the gel electrophoresis SDS-PAGE and sequentially transferred to nitrocellulose membranes. After protein transfer, the immunostaining was initiated using a blocking solution containing 5% skimmed milk in TBS buffer (2.24 g/L Tris base and 8 g/L NaCl, pH 7.6) and 0.1% Tween-20 for 1 h at RT. Subsequently, nitrocellulose membranes with proteins were incubated in primary antibodies against GFAP, GDNF, S100 and glyceraldehyde-3-phosphate dehydrogenase GAPDH proteins overnight at 4 °C (Table 1). After that, membranes were incubated in their corresponding horseradish peroxidase-conjugated secondary antibodies for 2 h at RT (Table 1). The band intensity of the immunodetection was revealed using a Novex ECL Chemiluminescent Substrate Reagent Kit (Thermo Fisher Scientific, Waltham, MA, USA). The ChemiDoc MP imaging program was used for the image acquisition. The bands of the molecular weights for GFAP (50 kDa), GDNF (15 kDa) and S100 (9-13 kDa) were measured using ImageJ® version 1.43° software. Changes in the proteins expression in this study were normalized comparing with the level expression of GAPDH. The results were expressed in arbitrary units. The Western blot was performed according to do Nascimento et al. (2019) [48] and Vicentini et al. (2016) [52].

2.7. Statistical analysis

The statistical analysis was performed using Statistica 8.1 and GraphPad Prism 6.1, and expressed as mean ± standard error of the mean. The morphometric data were designed in Randomized Block Design, followed by the Fisher's Test. For the quantitative data, one-way ANOVA analysis of variance was performed, followed by the Fisher's Test. The $p < 0.05$ was considered significant.

3. Results

3.1. Volume of paw edema and intestinal area

The analysis of the intestinal area revealed significant effects ($F_{(4, 16)} = 3.1719$; $p = 0.04249$) in this study. Comparing the experimental groups, no statistically significant differences for the jejunal area of the small intestine, except for A group that displayed a intestinal area atrophy of 10% compared to C group ($p < 0.05$; Table 2).

Considering the analysis of volume of the left hind paw edema, significant results were also obtained on days 0 ($F_{(4, 16)} = 4.4332$; $p = 0.01334$), 1st ($F_{(4, 16)} = 36.621$; $p = 0.00001$), 3rd ($F_{(4, 16)} = 34.138$; $p = 0.00001$) and 6th ($F_{(4, 16)} = 56.450$; $p = 0.00001$). A group displayed an increase of the paw volume ($p < 0.0001$) in relation to the control on days 1st, 3rd and 6th (Table 2). In these same days, there were reductions in the paw volume for the AI ($p < 0.05$), AQ ($p < 0.05$) and AIQ ($p < 0.0001$) groups compared to A group (Table 2).

3.2. Density and morphometry for the HuC/D-IR neurons and S100-IR glial cells

The analysis of the density of the HuC/D-IR neurons displayed significant values in the myenteric ($F_{(4, 741)} = 17.485$; $p = 0.00001$) and submucosal ($F_{(4, 741)} = 15.306$; $p = 0.00001$) plexuses. Regarding the density of the S100-IR EGC, significant results were also obtained in the myenteric ($F_{(4, 741)} = 50.821$; $p = 0.00001$) and submucosal ($F_{(4, 741)} = 127.81$; $p = 0.00001$) plexuses. Comparing the groups, the density of the HuC/D-IR neurons in the myenteric and submucosal plexuses reduced 35.9% and 26.9% in arthritic group, respectively (vs C; $p < 0.0001$; Fig. 1A). The density of the S100-IR EGC in the myenteric and submucosal plexuses also displayed a decreased number of 43.7% and 72.4% in A group, respectively (vs C; $p < 0.0001$; Fig. 1B). In the AI, AQ and AIQ groups, there was a density preservation of the HuC/D-IR myenteric neurons of 19%, 43% and 22% compared to A group, respectively (vs A; 0.0001; Fig. 1A). In the submucosal plexus, a neuronal preservation of the HuC/D-IR neurons was observed in AQ (16%; $p < 0.003$) and AIQ (12%; $p < 0.05$) groups (vs A; Fig. 1B). In these same groups, AI, AQ and AIQ groups yielded a density preservation of S100-IR EGC in the myenteric plexus of 29.3%, 72% and 39.7%, respectively (vs A; $p < 0.0001$; Fig. 1B). In the submucosal plexus, the preservation of the S100-IR cells was much more expressive: 106% (AI), 156% (AQ) and 138% (AQ) (vs A; $p < 0.0001$; Fig. 1B). For both HuC/D and S100 markers, the cellular densities in the AQ group were similar to those observed in control ($p > 0.05$).

Evaluating the analysis of the areas of the neuronal bodies, significant values were obtained in the myenteric ($F_{(4, 2491)} = 61.381$; $p = 0.00001$) and submucosal ($F_{(4, 2491)} = 9.6369$; $p = 0.00001$) plexuses. For the glial somatic area of the EGC, significant effects were also observed in the myenteric ($F_{(4, 2491)} = 38.117$; $p = 0.00001$) and submucosal ($F_{(4, 2491)} = 24.290$; $p = 0.00001$) plexuses. Comparing the experimental groups, an increased area of 21% and 18.7% was observed in the myenteric plexus for the neurons and EGC, respectively (A

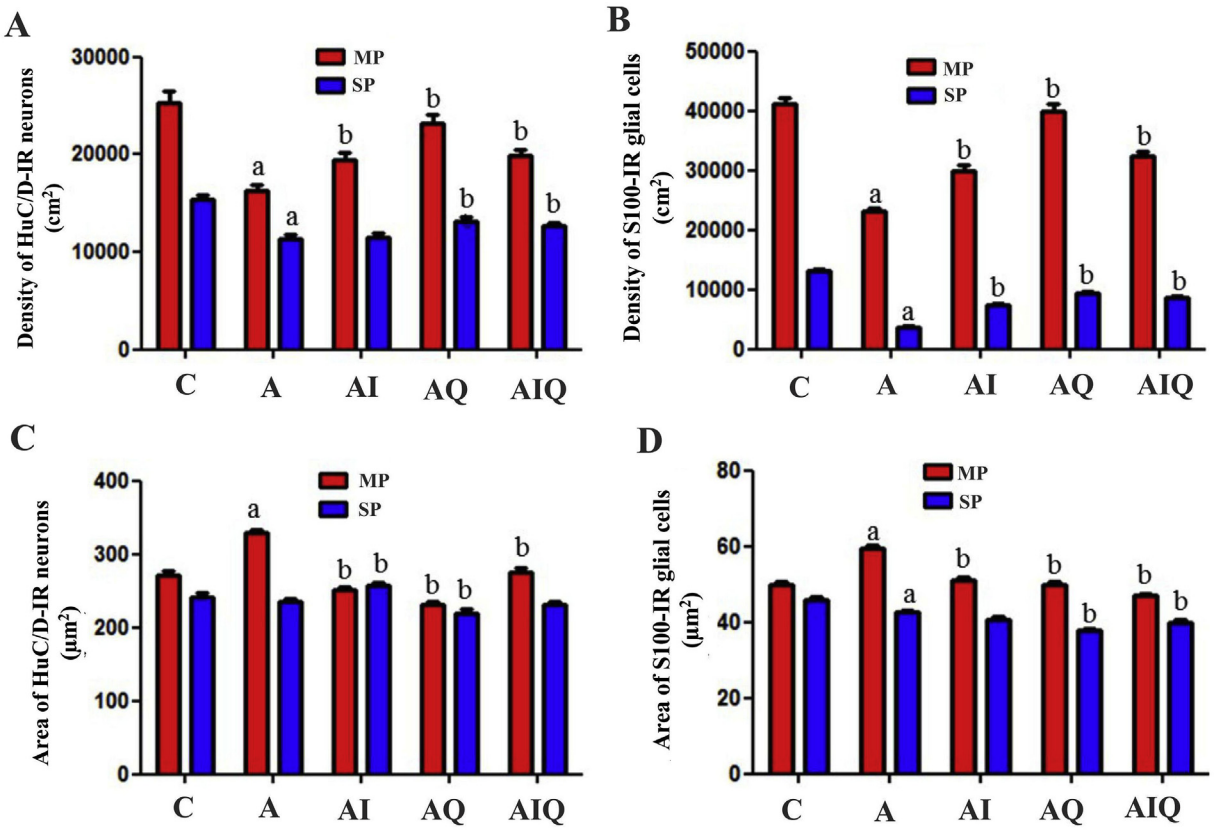

Fig. 1. Results of the quantitative analysis of HuC/D-IR neurons (A) and CGE-IR glial cells (B) expressed in cm^2; and the morphometric analysis of the HuC/D-IR neurons (C) and CGE-IR glial cells (D) expressed in μm^2 in the myenteric (MP) and submucosal (SP) plexuses of the jejunum. Experimental groups: control (C), arthritic (A), arthritic treated with 17.5 mg/kg ibuprofen (AI), arthritic treated with 50 mg/kg quercetin (AQ) and arthritis treated with 50 mg/kg quercetin and 17.5 mg/kg ibuprofen (AIQ). [a] = significant in comparison to the control group ($p < 0.05$) and [b] = significant in comparison to the arthritic group ($p < 0.05$). Results are expressed as mean ± standard error. n = 5 animals per group.

vs. C; $p < 0.0001$; Fig. 1C and D). However, the arthritis resulted in a 7.4% reduction of cellular area of the S100-IR EGC in the submucosal plexus (A vs. C; $p < 0.0001$; Fig. 1D).

In the treated groups (AI, AQ and AIQ), decreased cellular body areas were observed for the HuC/D-IR neurons (23.4%, 29.7% and 19.1%, respectively; $p < 0.0001$; Fig. 1C) and the S100-IR EGC (13.7%, 16.3% and 21%, respectively; $p < 0.0001$; Fig. 1D) in the myenteric plexus in comparison to A group. In the submucosal plexus, an increased cellular body area (9.7%; $p < 0.0001$) of the HuC/D-IR neurons in the AI group was observed, whereas AQ group displayed a decreased somatic area (6.8%; $p < 0.05$) for these neurons (vs A; $p < 0.01$; Fig. 1C). Reductions for the S100-IR EGC (vs A; Fig. 1D) were seen in AIQ (6.1%; $p < 0.05$) and AQ (10.9%; $p < 0.0001$) groups in the submucosal plexus. Representative images of S100-IR EGC and HuC/D-IR neurons are shown in Fig. 2 and Fig. 3.

3.3. Occupancy area by the GFAP-IR intermediate filaments and quantification of the GFAP-expressing EGC in the myenteric plexus

Significant effects were obtained for the analysis of the GFAP-IR intermediate filaments ($F_{(4, 491)} = 22.103$; $p = 0.00001$) and density of the GFAP-expressing EGC ($F_{(4, 491)} = 28.105$; $p = 0.00001$). Regarding the experimental groups, arthritis (group A) resulted in a decrease of 34% ($p < 0.0001$) and 49% ($p < 0.0001$) for the occupancy area by the GFAP-IR intermediate filaments (Fig. 4A and C) and density of the GFAP-expressing EGC, respectively (Fig. 4B and C). Comparing the treatment effects to the arthritic group, increases of the occupancy area by the GFAP-IR gliofilaments were observed for the AQ (66%) and AIQ (72%) groups (vs A; $p < 0.0001$; Fig. 4A). For the GFAP-expressing EGC, enhances of 62%, 113% and 89% were observed for the AI, AQ and AIQ groups, respectively (vs A; $p < 0.0001$; Fig. 4B). For both analyzes, quercetin treatment (AQ) displayed similar values to the control ($p > 0.05$).

3.4. Expression of the GFAP, S100 and GDNF proteins

Statistically significant values were observed regarding the analysis of the expressions of the GFAP ($F_{(4, 16)} = 6.5844$; $p = 0.00249$), S100 ($F_{(4, 16)} = 3.3976$; $p = 0.03416$) and GDNF ($F_{(4, 16)} = 5.5467$; $p = 0.00536$) proteins. Comparing the experimental groups, there was a reduction of the GDNF (33.5%; $p < 0.0001$; Fig. 5C) and GFAP (18%; $p < 0.0001$; Fig. 5A) expressions in the arthritic animals (A group) compared to C group. In the treated group (AI, AQ and AIQ), there was an increase of the GFAP expressions in 20.2%, 29% and 34%, respectively (vs A; $p < 0.05$; Fig. 5A). For the GDNF expressions, enhances of 32% ($p < 0.0001$), 72% ($p < 0.05$) and 60% ($p < 0.05$) were found for AI, AQ and AIQ groups, respectively (vs A; Fig. 5C). In the AI, AQ and AIQ groups, decreased S100 expressions of 9% ($p < 0.05$), 4.8% ($p < 0.0001$) and 40% ($p < 0.05$) were evidenced (vs A; Fig. 5B).

3.5. Quantification of the CD45 and CD20 lymphocytes and length of the villi and total wall thickness

Significant effects were observed for the density of the CD45 ($F_{(4, 741)} = 43.860$; $p = 0.00001$) and CD20 ($F_{(4, 741)} = 88.741$; $p = 0.00001$) lymphocytes. A group exhibited remarkable increases of the density of the CD45 (91%) and CD20 (159%) lymphocytes per villus compared to C group (Fig. 6A; $p < 0.0001$). Evaluating the CD45

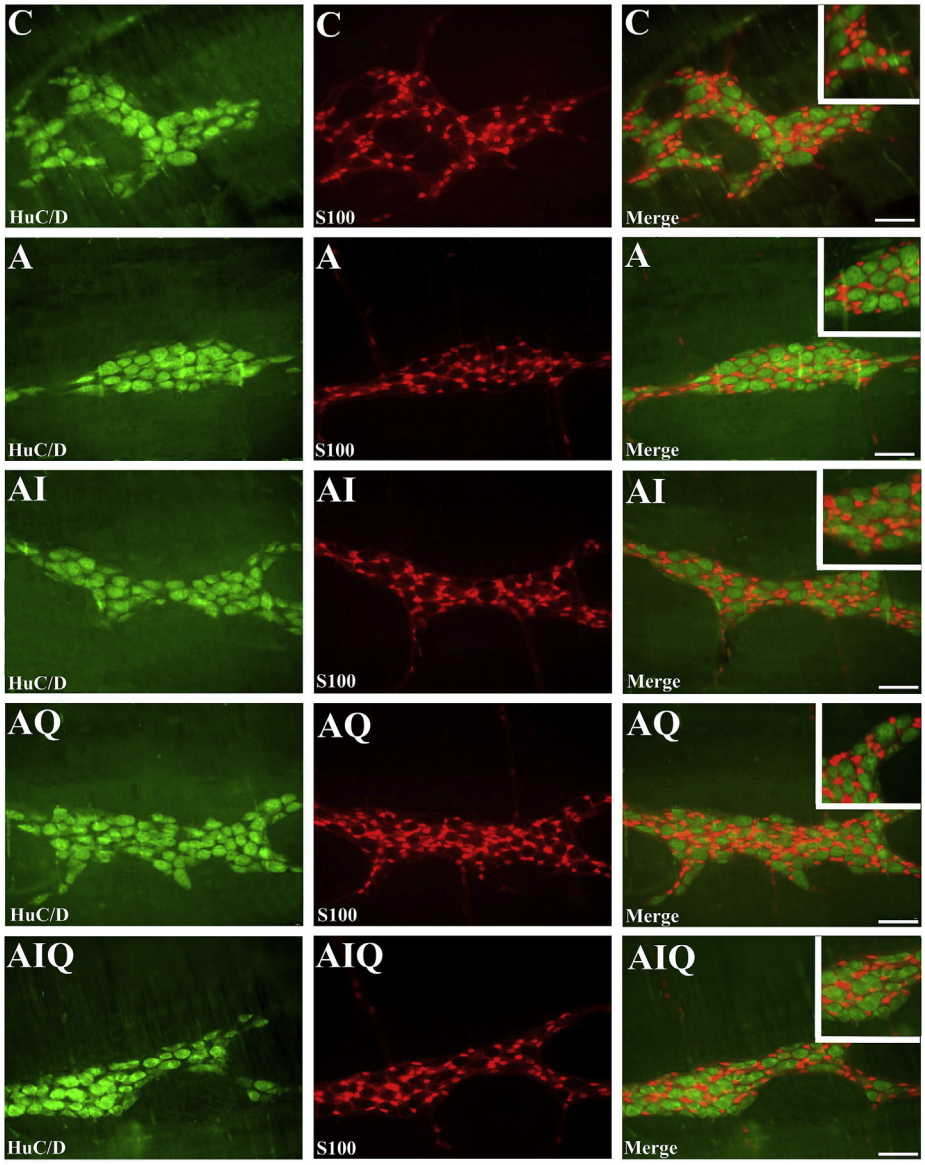

Fig. 2. Immunostaining for the HuC/D-IR neurons and S100-IR glial cells, and merge of both markers in the myenteric plexus of the jejunum of arthritic rats. Experimental groups: control (C), arthritic (A), arthritic treated with 17.5 mg/kg ibuprofen (AI), arthritic treated with 50 mg/kg quercetin (AQ) and arthritis treated with 50 mg/kg quercetin and 17.5 mg/kg ibuprofen (AIQ). Scale bar = 20 μm.

lymphocyte density of the treated groups in relation to A group (Fig. 6A), decreased densities of 33% ($p < 0.0001$; AI group) and 29% ($p < 0.0001$; AQ group) were observed for the total CD45 lymphocytes, whereas AIQ group showed a 11% higher density of these lymphocytes ($p < 0.05$). For the CD20 lymphocytes (Fig. 6A), density reductions of 40% and 41% were observed for the AI and AQ groups (vs A; $p < 0.0001$), respectively.

Statistically significant results values were also obtained for the analysis of the villus height ($F_{(4, 741)} = 29.767$; $p = 0.00001$) and total wall length ($F_{(4, 741)} = 45.816$; $p = 0.00001$). A group displayed a decrease of 11% villus height and 8% total wall size (vs C; $p < 0.0001$; Fig. 6B). Furthermore, increased villus heights were found in AI (17.2%), AQ (6%) and AIQ (14.8%) groups (vs A; $p < 0.0001$; Fig. 6B). Regarding the total thickness of jejunal mucosa, AI and AIQ groups yielded an increase of 12% and 5.9% in its length, respectively (vs A; $p < 0.0001$; Fig. 6B). Photomicrographs of the immunostainings for CD45 and CD20 are shown in Fig. 6C.

4. . Discussion

In this study, the chronic and severe model of CFA-induced arthritis demonstrated that the extra-articular and systemic effects of RA negatively affected the cellular components of the SNE and intestinal mucosa. These findings deserve the researchers' attention since until now few studies have demonstrated cellular and molecular impairment on ENS and GIT induced by the RA in order to uncover how this disease results in some gastrointestinal symptoms in arthritic patients (e.g. abdominal pain, which is considered almost universal, whereas nausea, vomiting or diarrhea occur in about one-third of patients) [56,57]. The establishment of this inflammatory model was confirmed by the increase of the left hind paw edema of these animals on 1st, 3rd and 6th days. Since the occurrence of systemic manifestations mainly occurs in severe arthritic disease [3], in this study, RA resulted in remarkable neurodegeneration in the jejunum of the arthritic rats due to the decreased density of the enteric neurons and the EGC in the myenteric and submucosal plexuses, which may affect the functioning of the ENS and GIT. The RA-induced effects on ENS should also be investigated in the

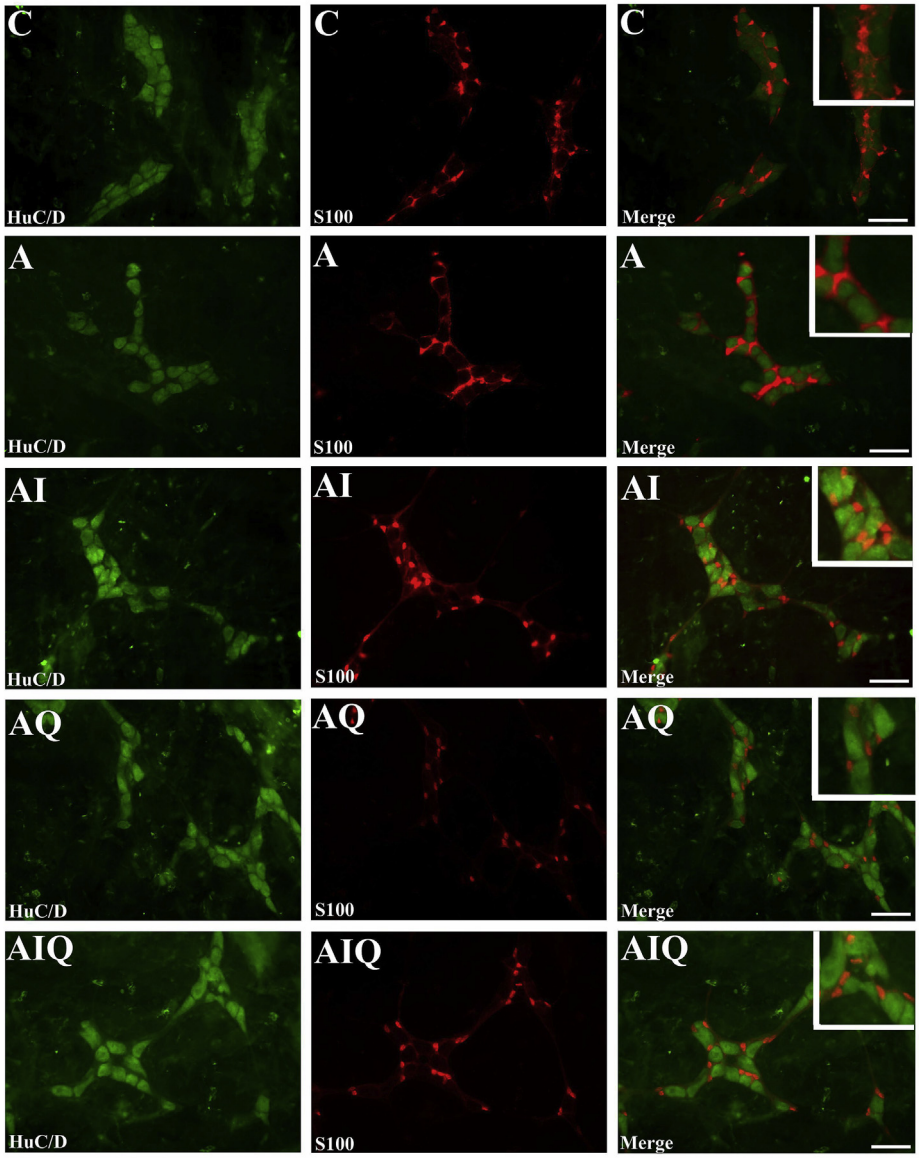

Fig. 3. Immunostaining for the HuC/D-IR neurons and S100-IR glial cells, and merge of both markers in the jejunal submucosal plexus of arthritic rats. Experimental groups: control (C), arthritic (A), arthritic treated with 17.5 mg/kg ibuprofen (AI), arthritic treated with 50 mg/kg quercetin (AQ) and arthritis treated with 50 mg/kg quercetin and 17.5 mg/kg ibuprofen (AIQ). Scale bar = 20 μm.

acute phase for future studies in order to determine the severity in this stage on ENS.

The increased body area of the neurons and EGC in the myenteric plexus of the arthritic animals (A group) observed in this study suggests a beneficial compensatory effect due to an increase in the cellular enzymatic machinery in order to reestablish the gastrointestinal activity the closest to the ideal due to neuronal and glial loss [36,58,59]. However, in the submucosal plexus, only EGC displayed reduction of their cellular area, which may indicate a deleterious gliopathic effect induced by the arthritic disease, resulting in a lower enzymatic activity of these cells [36,59]. Phenotypic changes of the EGC and enteric neurons indicate the presence of cellular plasticity to suit changes in environmental conditions that the ENS is exposed [23]. Furthermore, the decrease of the glial network, GFAP expression and GFAP-expressing EGC indicates that these cells are not compensating their glial density reduction and neuronal loss, thus being more susceptible to the damages caused by the arthritic disease. It is well-known that these cells create a protective microenvironment that provides support to the neurons through the expansion of these gliofilaments and synthesis of neurotrophic factors (e.g. GDNF), preventing the neuronal death [23,59]. These EGC play a crucial structural role for the enteric neurons involving their cellular bodies and axons [27,56]. In addition, EGC are responsible for responding to mechanical and exogenous stimuli, increasing the production of GFAP-IR intermediate filaments to provide a structural and physical barrier against cytotoxic and immunological effects on enteric neurons [23].

In line with the results described above, the lower GFAP and GDNF expressions observed by the RA (A group) probably occurred due to the substantial glial loss in this study. Furthermore, the increased expression of the S100 protein, even considering the reduction of the EGC in both ganglionated plexuses, may be explained by the increase of the glial somatic area in the myenteric plexus where there are higher glial density than the submucosal plexus. Despite of the decrease of glial bodies in submucosal plexus, a higher production of S100 probably occurred in the cytoplasm and nucleus [14,15,23]. However, the increased expression of this protein may activate the inflammatory and immune process through the production of pro-inflammatory cytokines by the EGC but, in its downregulation, S100 may be beneficial reducing

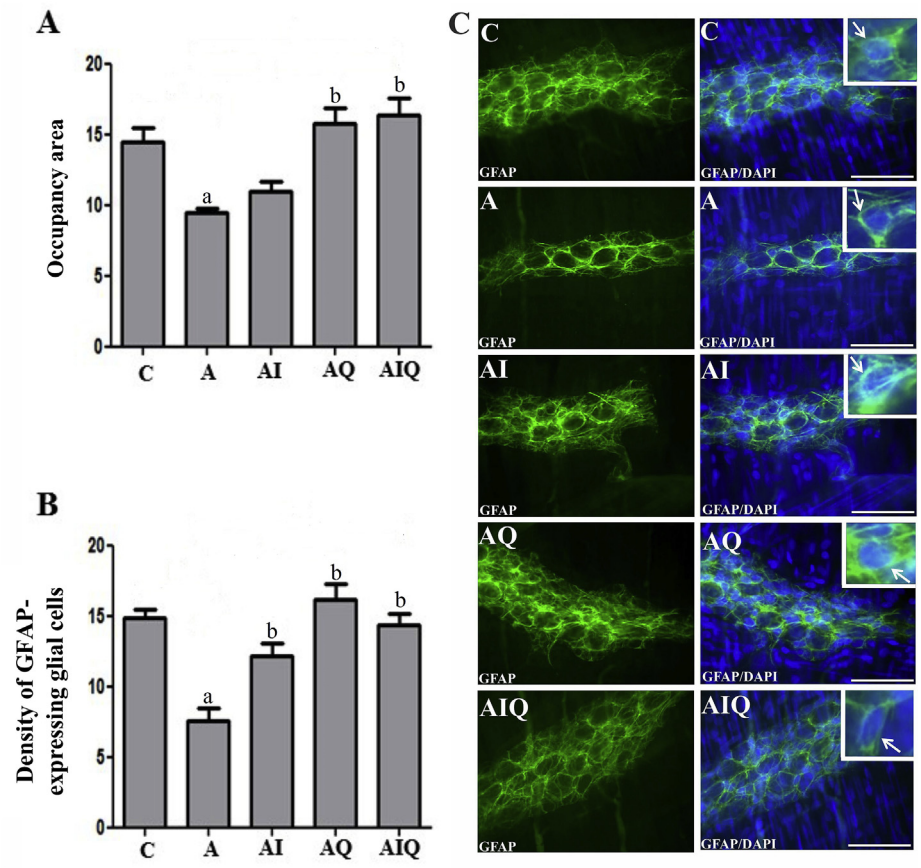

Fig. 4. Occupancy area by the intermediate filaments of GFAP (A) and quantification of GFAP-expressing glial cells (B) in the myenteric plexus. Fig. C illustrates the immunostaining for GFAP-IR intermediate filaments and their merge with DAPI in the myenteric plexus of the jejunum of arthritic rats. Experimental groups: control (C), arthritic (A), arthritic treated with 17.5 mg/kg ibuprofen (AI), arthritic treated with 50 mg/kg quercetin (AQ) and arthritic treated with 50 mg/kg quercetin and 17.5 mg/kg ibuprofen (AIQ). Results are expressed as mean ± standard error. [a] = significant in comparison to the control group ($p < 0.05$) and [b] = significant in comparison to the arthritic group ($p < 0.05$). n = 5 rats per group. Scale bar = 40 μm.

the intestinal inflammation and increasing the synthesis of GFAP and GDNF [60–63]. For this reason, the increased S100 expression may indicate an intensification of the inflammatory bowel process, which probably justifies the presence of the remarkable inflammation of the intestinal mucosa observed by the expressive increase of the B and total lymphocytes in arthritic animals. Furthermore, the decreases of the villus height, total wall thickness and the intestinal area of the jejunum suggest atrophic processes, which may indicate a reduction in intestinal absorption capacity [64]. Inflammation of the small and large intestine has been recently described in arthritic patients [52]. Several studies on the ENS and mucosa have been carried out using models of parasitic infection (e.g. Chagas disease, toxoplasmosis, schistosomiasis, etc.), diabetes, aging, blood hypoperfusion, obesity, cancer, etc. Surprisingly, based on the results found in this study, the severe and chronic arthritic disease displays a high relevance in the area of gastroenterology.

Regarding the quercetin effects (AQ group) on ENS and intestinal mucosa, our results indicated that quercetin treatment at a dose of 50 mg/kg resulted in protective effects compared to the arthritic group, reestablishing almost all parameters evaluated in this study affected by the disease. These results show that quercetin promoted neuro- and glioprotective effects on the ENS, as well as anti-inflammatory actions on the intestinal mucosa. Possibly, antioxidant effects may have also occurred since the reduction of glial and neuronal somatic area, even comparing to the healthy control, suggests protective antioxidant effects, decreasing the amount of intracellular free radicals as a beneficial compensatory effect [36]. Such antioxidant effects are directly responsible for preventing the neuronal and glial loss [36–39].

Given the antioxidant and neuroprotective properties of the quercetin [36–40], several studies have been conducted in diabetic animals showing protective effects of the quercetin on the population of the enteric neurons and/or glial cells using quercetin supplementation in water at doses of 200 mg/kg [37,38] and 40 mg/kg [36,39]. The dose of 50 mg/kg per gavage in this *in vivo* arthritic model showed superior results on the ENS than quercetin supplementation in water previously

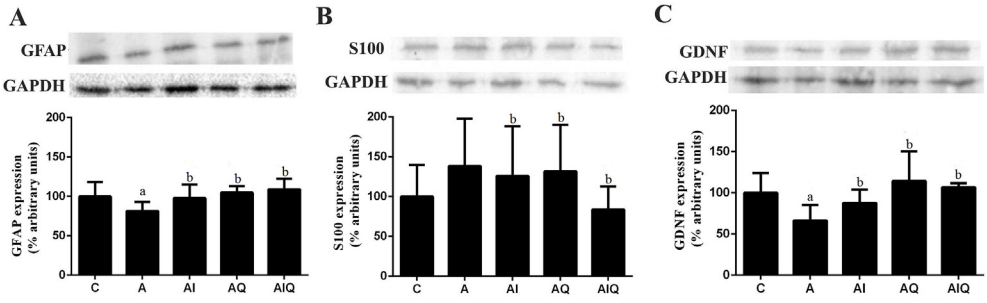

Fig. 5. Representative immunoblots for the following proteins: GFAP (A), S100 (B) and GDNF (C) and standard GAPDH proteins used for normalization. The results of Western blot analyzes were expressed as the percentage of arbitrary units. n = 4 rats per group. Groups: control (C), arthritic (A), arthritic treated with 17.5 mg/kg ibuprofen (AI), arthritic treated with 50 mg/kg quercetin (AQ) and arthritis treated with 50 mg/kg quercetin and 17.5 mg/kg ibuprofen (AIQ). Results expressed as mean ± standard error. [a] = significant in comparison to the control group ($p < 0.05$) and [b] = significant in comparison to the arthritic group ($p < 0.05$). n = 4 rats.

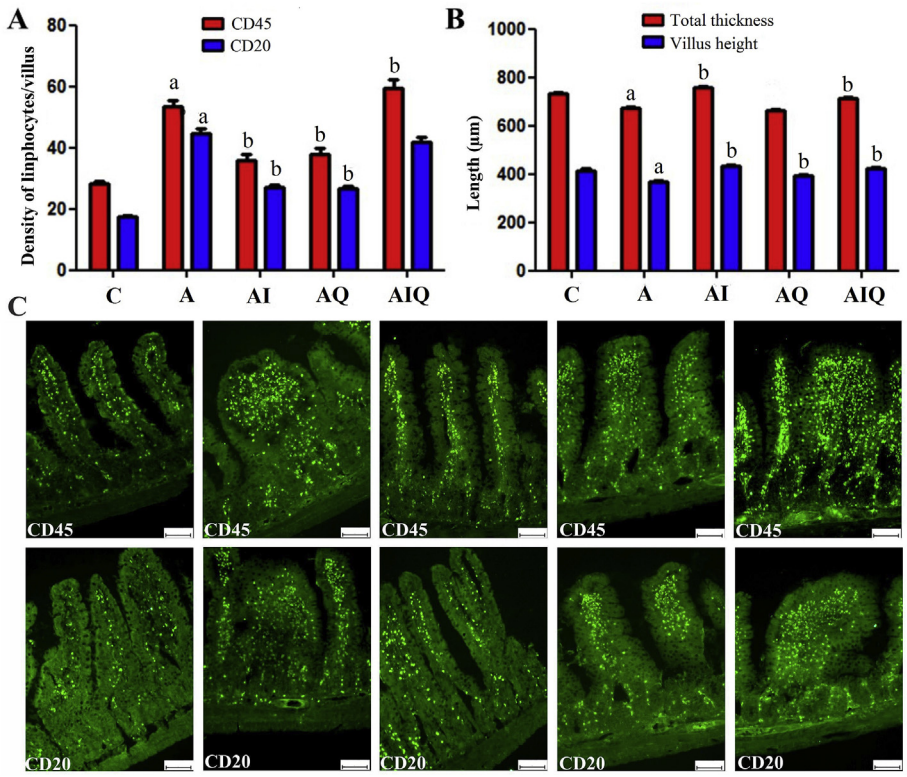

Fig. 6. Quantification of CD45 and CD20 (A) lymphocytes in the villi of the intestinal mucosa and measurement of the villus height and total wall thickness of the jejunum (B). Results are expressed as mean ± standard error. Representative immunostainings (C) of lymphocyte density of CD45 (total lymphocytes) and CD20 (B lymphocytes), and measurements of villus height and total thickness of jejunal mucosa of arthritic rats. Experimental groups: control (C), arthritic (A), arthritic treated with 17.5 mg/kg ibuprofen (AI), arthritic treated with 50 mg/kg quercetin (AQ) and arthritis treated with 50 mg/kg quercetin and 17.5 mg/kg ibuprofen (AIQ). [a] = significant in comparison to the control group ($p < 0.05$) and [b] = significant in comparison to the arthritic group ($p < 0.05$). n = 5 animals per group. Scale bar = 10 µm.

used for diabetic rats. Based on anti-rheumatic effects and anti-inflammatory actions of this flavonoid [33–35], quercetin treatments by gavage demonstrated anti-inflammatory effects on the joints [40,65] and other systemic organs affected by the disease, such as the liver and lung [38]. Our results displayed reduction of the paw edema by the quercetin treatment (AQ group) on the days 1st, 3rd and 6th, indicating anti-inflammatory effects. For these reasons, quercetin supplementation by the humans may avoid cartilage and joint damages and protect the GIT. Furthermore, quercetin treatment used alone may result in superior and inferior results compared to other studies depending on the dose, time and *in vivo* model. Aiming to search new promising therapies in order to simultaneously protect the ENS and joint inflammation, the efficacy of the quercetin was evaluated alone and in combination with ibuprofen in this research. In addition, new formulations using quercetin (e.g. nanoparticle-delivered quercetin, quecertin-loaded microcapsules, etc) have been developed due to the multifaceted therapeutic applications of this flavonoid that gradually control its release in the small intestine. New combinatory therapies using quercetin and anti-rheumatic drugs may be performed (e.g. changes of the doses of each substance, treatment time, combinations with other antirheumatic drugs used by the humans, etc). Co-administration of antioxidants with other antirheumatic drugs already present in the market (e.g. DMARS and other NSAIDs) may reach higher prognosis against arthritis-induced harmful effects (e.g. joint inflammation and enteric neurodegeneration). In this study, quercetin treatment in healthy animals was not evaluated since studies have shown that quercetin, depending on the dose and time of administration, may result in pro-oxidant and toxic effects [64–69].

Treatment with ibuprofen, the commercially available anti-inflammatory drug and used by the humans, at the standard dose of 17.5 mg/kg as well as the combination of ibuprofen and quercetin displayed beneficial results compared to AQ, although these effects were lesser expressive. The results showed that the treatment alone with ibuprofen confirmed its anti-inflammatory activity on the ENS and the intestinal mucosa. Aiming to find combinatorial therapies with additive and synergistic effects, in this work, combined treatment (quercetin and ibuprofen) showed inferior results than those obtained by the treatment with quercetin alone in jejunum, in addition to being unable to reduce intestinal inflammation of the jejunal mucosa, even considering anti-inflammatory properties of these two substances. Lower doses of both drugs in combination could be assessed to obtain synergistic effects in the evaluated parameters.

5. Conclusion

In summary, this study confirmed that rheumatoid arthritis results in important neurodegenerative processes on the ENS of the jejunum and inflammatory process in the intestinal mucosa of arthritic rats. These findings are relevant in the gastroenterology for the correct interpretation of GIT symptoms that arthritic patients suffer. Treatment with quercetin alone reversed almost all degenerative effects on ENS, possibly due to its antioxidant, anti-inflammatory and neuroprotective roles. Treatment with ibuprofen alone showed effective anti-inflammatory effects, but lower expressive effects than the treatment with quercetin alone. The combined treatment of quercetin with ibuprofen yielded beneficial results against the arthritic neuropathy but did not reduce the inflammatory process in the jejunal mucosa.

Declaration of competing InterestCOI

The authors declare that they have no competing interests.

Funding

This work was supported by CAPES (Coordenação de Aperfeiçoamento de Pessoal de Nível Superior)

Acknowledgements

We have no acknowledgements in this study.

References

[1] J.S. Smolen, D. Aletha, Rheumatoid arthritis therapy reappraisal strategies, opportunities and challenges, Nat. Rev. Rheumatol. 11 (2015) 276–289, https://doi.org/10.1038/nrrheum.2015.8.

[2] I. Rudan, S. Sidhu, A. Papana, S.J. Meng, Y. Xin–Wei, W. Wang, R.M. Campbell–Page, A.R. Demaio, H. Nair, D. Sridhar, E. Theodoratou, B. Dowman, D. Adeloye, A. Majeed, J. Car, H. Campbell, W. Wang, K.Y. Chan, Prevalence of rheumatoid arthritis in low– and middle–income countries: a systematic review and analysis, J Glob Health 5 (2015) 1–10, https://doi.org/10.7189/jogh.05.010409.

[3] M. Cojocaru, I.M. Cojocaru, I. Silosi, C.D. Vrabie, Gastrointestinal manifestations in systemic autoimmune diseases, Maedica (Bucharest, Romania) 6 (1) (2011) 45–51 https://www.ncbi.nlm.nih.gov/pubmed/21977190.

[4] E.C. Ebert, K.D. Hagspiel, Gastrointestinal and hepatic manifestations of rheumatoid arthritis, Dig. Dis. Sci. 56 (2) (2011) 295–302, https://doi.org/10.1007/s10620-010-1508-7.

[5] A. Lerner, T. Matthias, Rheumatoid arthritis celiac disease relationship: joints get that gut feeling, Autoimmun. Rev. 14 (11) (2015) 1038–1047, https://doi.org/10.1016/j.autrev.2015.07.007.

[6] P. Rawla, Cardiac and vascular complications in rheumatoid arthritis, Reumatologia 57 (2019) 27–36, https://doi.org/10.5114/reum.2019.83236.

[7] M. Veselinovic, N. Barudzic, M. Vuletic, V. Zivkovic, A. Tomic-Lucic, D. Djuric, V. Jakovljevic, Oxidative stress in rheumatoid arthritis patients: relationship to diseases activity, Mol. Cell. Biochem. 391 (2014) 225–232, https://doi.org/10.1007/s11010-014-2006-6.

[8] G.S. Firestein, I.B. McInnes, Immunopathogenesis of rheumatoid arthritis, Immunity 46 (2) (2017) 183–196, https://doi.org/10.1016/j.immuni.2017.02.006.

[9] C.M. Quiñonez-Flores, S.A. González-Chávez, A.D.R. Nájera, C. Pacheco-Tena, Oxidative stress relevance in the pathogenesis of the rheumatoid arthritis: a systematic review, BioMed Res. Int. (2016) 1–14, https://doi.org/10.1155/2016/6097417 2016.

[10] G. Albani, S. Ravaglia, L. Cavagna, R. Caporali, C. Montecucco, Clinical and electrophysiological evaluation of peripheral neuropathy in rheumatoid arthritis, J. Peripher. Nerv. Syst. (11) (2006) 174–175, https://doi.org/10.1111/j.1085-9489.2006.00084.x.

[11] V. Agarwal, R. Singh, S. Chauhan, A. Tahlan, C.K. Ahuja, A clinical, electrophysiological, and pathological study of neuropathy in rheumatoid arthritis, Clin. Rheumatol. (27) (2007) 841–844, https://doi.org/10.1111/j.1085-9489.2006.00084.x.

[12] M.K. Sim, D. Kim, J. Yoon, D.H. Park, Y. Kim, Assessment of peripheral neuropathy in patients with rheumatoid arthritis who complain of neurologic symptoms, Ann Rehabil Med(Seoul, Korea) 38 (2) (2014) 249–255, https://doi.org/10.5535/arm.2014.38.2.249.

[13] I.D. Souza, J.S. Ribeiro, C.A. Bersani-Amado, J.N. Zanoni, Analysis of myosin-V immunoreactive myenteric neurons from arthritic rats, Arq. Gastroenterol. 48 (3) (2011), https://doi.org/10.1590/S0004-28032011000300010 2205-10.

[14] J.B. Furness, Structure of the Enteric Nervous System, the Enteric Nervous System, Malden, Blackwell Pub, Melbourne, Australia, 2006, pp. 1–28.

[15] J.B. Furness, The enteric nervous system and neurogastroenterology, Nat. Rev. Gastroenterol. Hepatol. 9 (5) (2012), https://doi.org/10.1038/nrgastro.2012.32 286-94.

[16] R. de Giorgio, F. Giancola, E. Boschetti, H. Abdo, B. Lardeux, M. Neunlist, Enteric glia and neuroprotection: basic and clinical aspects, Am. J. Physiol. Gastrointest. Liver Physiol. 303 (8) (2012) 887–893, https://doi.org/10.1152/ajpgi.00096.2012.

[17] M. Neunlist, L.V. Landeghem, M.M. Mahé, P. Derkinderen, S.B. des Varannes, M. Rolli-Derkinderen, The digestive neuronal–glial–epithelial unit: a new actor in gut health and disease, Nat. Rev. Gastroenterol. Hepatol. 10 (2) (2013) 90–100.

[18] J.B. Furness, B.P. Callaghan, L.R. Rivera, H.J. Cho, The enteric nervous system and gastrointestinal innervation: integrated local and central control, Adv. Exp. Med. Biol. 817 (2014) 39–71, https://doi.org/10.1007/978-1-4939-0897-4_3.

[19] F. Ochoa-Cortes, F. Turco, A. Linan-Rico, S. Soghomonyan, E. Whitaker, S. Wehner, Enteric glial cells: a new frontier in neurogastroenterology and clinical target for inflammatory bowel diseases, Inflamm. Bowel Dis. 22 (2016) 433–449, https://doi.org/10.1097/MIB.0000000000000667.

[20] M. Rao, D. Rastelli, L. Dong, S. Chiu, W. Setlik, M.D. Gershon, G. Corfas, Enteric glia regulate gastrointestinal motility but are not required for maintenance of the epithelium in mice, Gastroenterology 153 (4) (2017) 1068–1081, https://doi.org/10.1016/j.brainresbull.2017.03.011.

[21] V. Grubišić, A. Verkhratsky, R. Zorec, V. Parpura, Enteric glia regulate gut motility in health and disease, Brain Res. Bull. 136 (2018) 109–117, https://doi.org/10.1016/j.brainresbull.2017.03.011.

[22] P. Luo, D. Liu, C. Li, W.X. He, C.L. Zhang, M.J. Chang, Enteric glial cell activation protects enteric neurons from damage due to diabetes in part via promotion of neurotrophic factor release, Neuro Gastroenterol. Motil. 30 (10) (2018) e13368, https://doi.org/10.1111/nmo.13368.

[23] S. Valès, M. Touvron, L. Van Landeghem, Enteric glia: diversity or plasticity? Brain Res. 1693 (Pt B) (2018) 140–145, https://doi.org/10.1016/j.brainres.2018.02.001.

[24] B.D. Gulbransen, K.A. Sharkey, Novel functional roles for enteric glia in the gastrointestinal tract, Nat. Rev. Gastroenterol. Hepatol. 9 (11) (2012) 625–632, https://doi.org/10.1038/nrgastro.2012.138.

[25] Y. Yan-Bo, L. Yan-Qing, Enteric glial cells and their role in the intestinal epithelial barrier, World J. Gastroenterol. 20 (32) (2014) 11273–11280, https://doi.org/10.3748/wjg.v20.i32.11273.

[26] C. Cirillo, G. Sarnelli, G. Esposito, F. Turco, L. Steardo, R. Cuomo, S100B protein in the gut: the evidence for enteroglial-sustained intestinal inflammation, World J. Gastroenterol. 17 (10) (2011) 1261–1266, https://doi.org/10.3748/wjg.v17.i10.1261.

[27] E. Capoccia, C. Cirillo, S. Gigli, M. Pesce, A. D'Alessandro, A. Cuomo, Enteric glia: a new player in inflammatory bowel diseases, Int. J. Immunopathol. Pharmacol. 28 (4) (2015) 443–451, https://doi.org/10.1177/0394632015599707.

[28] D.K. Zhang, F.Q. He, T.K. Li, X.H. Pang, D.J. Cui, Q. Xie, Glial-derived neurotrophic factor regulates intestinal epithelial barrier function and inflammation and is therapeutic for murine colitis, J. Pathol. 222 (2) (2010) 213–222, https://doi.org/10.1002/path.2749.

[29] W. Xiao, W. Wang, W. Chen, L. Sun, X. Li, GDNF is involved in the barrier-inducing effect of enteric glial cells on intestinal epithelial cells under acute ischemia reperfusion stimulation, Mol. Neurobiol. 50 (2014) 274–289, https://doi.org/10.1007/s12035-014-8730-9.

[30] M. Steinkamp, H. Gundel, N. Schulte, U. Spaniol, C. Pflueger, E. Zizer, G.B. von Boyen, GDNF protects enteric glia from apoptosis: evidence for an autocrine loop, BMC Gastroenterol. 12 (2012) 6, https://doi.org/10.1186/1471-230X-12-6.

[31] P. Kumar, S. Banik, Pharmacotherapy options in rheumatoid arthritis, Clin. Med. Insights Arthritis Musculoskelet. Disord. 6 (2013) 35–43, https://doi.org/10.4137/CMAMD.S5558.

[32] G. D'Andrea, Quercetin, A flavonol with multifaceted therapeutic applications? Fitoterapia 106 (2015) 256–271, https://doi.org/10.1016/j.fitote.2015.09.018.

[33] N. Haleagrahara, S. Miranda-Hernandez, M.A. Alim, L. Hayes, G. Bird, N. Ketheesan, Therapeutic effect of quercetin in collagen-induced arthritis, Biomed. Pharmacother. 90 (2017) 38–46, https://doi.org/10.1016/j.biopha.2017.03.026.

[34] J. Ji, Y. Lin, S. Huang, H. Zhang, Y. Diao, K. Li, Quercetin: a potential drug for adjuvant treatment of rheumatoid arthritis, Afr. J. Tradit., Complementary Altern. Med. 10 (2013) 418–421 https://www.ncbi.nlm.nih.gov/pubmed/24146468.

[35] C. Gardi, K. Bauerov, B. Stringa, V. Kuncirova, L. Slova, S. Ponist, Quercetin reduced inflammation and increased antioxidant defense in rat adjuvant arthritis, Arch. Biochem. Biophys. 583 (2015) 150–157, https://doi.org/10.1016/j.abb.2015.08.008.

[36] S.R. De Souza, M.H. de Miranda Neto, J.V. Martins Perles, F.C. Vieira Frez, I. Zignani, F.V. Ramalho, Antioxidant effects of the quercetin in the jejunal myenteric innervation of diabetic rats, Front. Med. 4 (2017) 8, https://doi.org/10.3389/fmed.2017.00008.

[37] P.E. Ferreira, C.R. Lopes, A.M. Alves, E.P. Alves, D.R. Linden, J.N. Zanoni, Diabetic neuropathy: an evaluation of the use of quercetin in the cecum of rats, World J. Gastroenterol. 19 (38) (2014) 6416–6426, https://doi.org/10.3748/wjg.v19.i38.6416.

[38] C.R. Lopes, P.E. Ferreira, J.N. Zanoni, A.M. Alves, E.P. Alves, N.C. Buttow, Neuroprotective effect of quercetin on the duodenum enteric nervous system of streptozotocin-induced diabetic rats, Dig. Dis. Sci. 57 (12) (2012) 3106–3115, https://doi.org/10.1007/s10620-012-2300-7.

[39] F.C.V. Frez, J.V.M.C. Perles, D.R. Linden, S.J. Gibbons, H.A. Martins, D.A. B Romualdo, S.R. de Souza, G.D.P. Bossolani, J.N. Zanoni, Restoration of density of interstitial cells of Cajal in the jejunum of diabetic rats after quercetin supplementation, Rev. Esp. Enferm. Dig. 109 (3) (2017) 190–195, https://doi.org/10.17235/reed.2016.4338/2016.

[40] L.G. Costa, J.M. Garrick, P.J. Roquè, C. Pellacani, Mechanisms of Neuroproctetion by Quercetin: Counteracting Oxidative Stress and More, Oxid Med Cell Longev, Washington, United States), 2016, pp. 1–10 2016.

[41] B.A. da Rocha, A.M. Ritter, F.Q. Ames, O.H. Gonçalves, F.V. Leimann, L. Bracht, M.R. Natali, R.K. Cuman, C.A. Bersani-Amado, Acetaminophen-induced hepatotoxicity: preventive effect of trans anethole, Biomed. Pharmacother. 86 (2017) 213–220, https://doi.org/10.1016/j.biopha.2016.12.014.

[42] E.S. Wisniewski-Rebecca, B.A. Rocha, L.A. Wiirzler, R.K. Cuman, C.A. Velazquez-Martinez, C.A. Bersani-Amado, Synergistic effects of anethole and ibuprofen in acute inflamatory response, Chem. Biol. Interact. 242 (2015) 247–253, https://doi.org/10.1016/j.cbi.2015.10.013.

[43] R.P. Aguiar, F.S. Aldawsari, L.A.M. Wiirzler, S.E. Silva-Filho, F.M.S. Silva-Comar, C.A. Bersani-Amado, C.A. Velazquez-Martinez, R.K.N. Cuman, Synthesis and biological evaluation of new tyrosol-salicylate derivatives as potential anti-inflammatory agents, Curr. Pharmaceut. Des. 23 (44) (2017) 6841–6848, https://doi.org/10.2174/1381612823666170602084553.

[44] C.P. Barbosa, L. Bracht, F.Q. Ames, F.M. de Souza Silva-Comar, R.P. Tronco, C.A. Bersani-Amado, Effects of ezetimibe, simvastatin, and their combination on inflammatory parameters in a rat model of adjuvant-induced arthritis, Inflammation 40 (2) (2017) 717–724, https://doi.org/10.1007/s10753-016-0497-x.

[45] C.M. Pearson, F.D. Wood, Studies of arthritis and other lesions induced in rats by the injection of mycobacterial adjuvant: VII. Pathologic details of the arthritis and spondylitis, Am. J. Pathol. 42 (1963) 73–95.

[46] R. Holmdahl, J.C. Lorentzen, S. Lu, P. Olofsson, L. Wester, J. Holmberg, U. Pettersson, Arthritis induced in rats with nonimmunogenic adjuvants as models for rheumatoid arthritis, Immunol. Rev. 184 (2001) 184–202.

[47] J.N. Zanoni, E.A. Tronchini, S.A. Moure, I.D. Souza, Effects of L-glutamine supplementation on the myenteric neurons from the duodenum and cecum of diabetic rats, Arq. Gastroenterol. 48 (1) (2011) 66–71, https://doi.org/10.1590/S0004-28032011000100014.

[48] C.P. do Nascimento Bonato Panizzon, M.H. de Miranda Neto, F.V. Ramalho, R. Longhini, J.C.P. de Mello, J.N. Zanoni, Ethyl acetate fraction from trichilia catigua confers partial neuroprotection in components of the enteric innervation of the jejunum in diabetic rats, Cell. Physiol. Biochem. 53 (1) (2019) 76–86, https://doi.org/10.33594/000000122.

[49] W. Liu, W. Yue, R. Wu, Effects of diabetes on expression of glial fibrillary acidic

protein and neurotrophins in rat colon, Auton. Neurosci. 154 (1–2) (2010) 79–83, https://doi.org/10.1016/j.autneu.2009.12.003.
[50] G.C. Preza, O.O. Yang, J. Elliott, P.A. Anton, M.T. Ochoa, T lymphocyte density and distribution in human colorectal mucosa,and inefficiency of current cell isolation protocols, PLoS One 10 (4) (2015) e0122723, , https://doi.org/10.1371/journal.pone.0122723.
[51] G.E. Vicentini, H.A. Martins, L. Fracaro, S.R.G. de Souza, K.P. da Silva Zanoni, T.N.X. Silva, F.P. Blegniski, F.A. Guarnier, J.N. Zanoni, Does l-glutamine-supplemented diet extenuate NO-mediated damage on myenteric plexus of Walker 256 tumor-bearing rats? Food Res. Int. 101 (2017) 24–34, https://doi.org/10.1016/j.foodres.2017.08.054.
[52] G.E. Vicentini, L. Fracaro, S.R.G. de Souza, H.A. Martins, F.A. Guarnier, J.N. Zanoni, Experimental cancer cachexia changes neuron numbers and peptide levels in the intestine: partial protective effects after dietary supplementation with L-glutamine, PLoS One 11 (9) (2016) e0162998, , https://doi.org/10.1371/journal.pone.0162998.
[53] G.B. von Boyen, M. Steinkamp, M. Reinshagen, K.H. Schäfer, G. Adler, J. Kirsch, Proinflammatory cytokines increase glial fibrillary acidic protein expression in enteric glia, Gut 53 (2) (2004) 222–228, https://doi.org/10.1136/gut.2003.012625.
[54] L. Fracaro, F.C. Frez, B.C. Silva, G.E. Vicentini, S.R. de Souza, H.A. Martins, J.N. Zanoni, Walker 256 tumor-bearing rats demonstrate altered interstitial cells of Cajal. Effects on ICC in the Walker 256 tumor model, Neuro Gastroenterol. Motil. 28 (1) (2016) 101–115, https://doi.org/10.1111/nmo.12702.
[55] M.M. Bradford, A rapid and sensitive method for the quantitation of microgram quantities of protein utilizing the principle of protein-dye binding, Anal. Biochem. 72 (1976) 248–254, https://doi.org/10.1006/abio.1976.9999.
[56] C. Pagnoux, A. Mahr, P. Cohen, L. Guillevin, Presentation and outcome of gastrointestinal involvement in systemic necrotizing vasculitides: analysis of 62 patients with polyarteritis nodosa, microscopic polyangiitis, Wegener granulomatosis, Churg-Strauss syndrome, or rheumatoid arthritis-associated vasculitis, Medicine (Baltim.) 84 (2) (2005) 115–128 https://www.ncbi.nlm.nih.gov/pubmed/15758841.
[57] E. Craig, L.C. Cappelli, Gastrointestinal and hepatic disease in rheumatoid arthritis, Rheum. Dis. Clin. N. Am. 44 (1) (2018) 89–111, https://doi.org/10.1016/j.rdc.2017.09.005.
[58] C. Hermes-Uliana, C.P. Panizzon, A.R. Trevizan, C.C. Sehaber, F.V. Ramalho, H.A. Martins, J.N. Zanoni, Is L-glutamine more effective than L-glutamine in preveting enteric diabetic neuropathy? Dig. Dis. Sci. 59 (5) (2014) 937–948, https://doi.org/10.1007/s10620-013-2993-2.
[59] A. Rühl, Glial regulation of neuronal plasticity in the gut: implications for clinicians, Gut 55 (5) (2005) 600–602, https://doi.org/10.1136/gut.2005.084426.
[60] K. Sharkey, Emerging roles for enteric glia in gastrointestinal disorders, J. Clin. Investig. 125 (3) (2015) 918–919, https://doi.org/10.1172/JCI76303.
[61] J.M. Coelho-Aguiar, A.C. Bon-Frauches, A.L.T. Gomes, C.P. Verıssimo, D.P. Aguiar, D. Matias, B.B.M. Thomasi, A.S. Gomes, G.A.C. Brito, V. Moura-Neto, The enteric glia. Identity and functions, Glia 63 (6) (2015) 921–935, https://doi.org/10.1002/glia.22795.
[62] G.B. T von Boyen, N. Schulte, C. Pflüger, U. Spaniol, C. Hartmann, M. Steinkamp, Distribution of enteric glia and GDNF during gut inflammation, BMC Gastroenterol. 11 (3) (2011) 1–8, https://doi.org/10.1186/1471-230X-11-3.
[63] C. Pochard, S. Coquenlorge, M. Freyssinet, P. Naveilhan, A. Bourreille, M. Neunlist, M. Rolli-Derkinderen, The multiple faces of inflammatory enteric glial cells: is Crohn's disease a gliopathy? Am. J. Physiol. Gastrointest. Liver Physiol. 315 (1) (2018) G1–G11, https://doi.org/10.1152/ajpgi.00016.2018.
[64] D. Shaw, K. Gohil, M.D. Basson, Intestinal mucosal atrophy and adaptation, World J. Gastroenterol. 18 (44) (2012) 6357–6375, https://doi.org/10.3748/wjg.v18.i44.6357.
[65] N. Haleagrahara, S. Miranda-Hernandez, M.A. Alim, L. Hayes, G. Bird, N. Ketheesan, Therapeutic effect of quercetin in collagen-induced arthritis, Biomed. Pharmacother. 90 (2017) 38–46, https://doi.org/10.1016/j.biopha.2017.03.026.
[66] M. Kessler, G. Ubeaud, L. Jung, Anti- and pro-oxidant activity of rutin and quercetin derivatives, J. Pharm. Pharmacol. 55 (1) (2003) 131–142, https://doi.org/10.1211/002235702559.
[67] E.J. Choi, G. H Kim, Quercetin accumulation by chronic administration causes the caspase-3 activation in liver and brain of mice, Biofactors 36 (3) (2010), https://doi.org/10.1002/biof.94 216-21.
[68] K.A. Youdim, M.Z. Qaiser, D.J. Begley, C.A. Rice-Evans, N.J. Abbott, Flavonoid permeability across an in situ model of the blood-brain barrier, Free Radic. Biol. Med. 36 (2004) 592–604, https://doi.org/10.1016/j.freeradbiomed.2003.11.023.
[69] M. Harwood, B. Danielewska-Nikiel, J.F. Borzelleca, G.W. Flamm, G.M. Williams, T.C. Lines, A critical review of the data related to the safety of quercetin and lack of evidence of in vivo toxicity, including lack of genotoxic/carcinogenic properties, Food Chem. Toxicol. 45 (2007) 2179–2205, https://doi.org/10.1016/j.fct.2007.05.015.